NOAA Technical Memorandum NESS 114

AN ATTITUDE PREDICTOR/TARGET SELECTOR

Washington, D.C.
February 1981

U.S. DEPARTMENT OF COMMERCE / National Oceanic and Atmospheric Administration / National Earth Satellite Service

(Continued from inside front cover)

NESS 87 Atlantic Tropical and Subtropical Cyclone Classifications for 1976. D. C. Gaby, J. B. Lushine, B. M. Mayfield, S. C. Pearce, K.O. Poteat, and F. E. Torres, April 1977, 13 pp. (PB-269-674/AS)

NESS 88 National Environmental Satellite Service Catalog of Products. Dennis C. Dismachek (Editor), June 1977, 102 pp. (PB-271-315/AS)

NESS 89 A Laser Method of Observing Surface Pressure and Pressure-Altitude and Temperature Profiles of the Troposphere From Satellites. William L. Smith and C. M. R. Platt, July 1977, 38 pp. (PB-272-660/AS)

NESS 90 Lake Erie Ice: Winter 1975-76. Jenifer H. Wartha, August 1977, 68 pp. (PB-276-386/AS)

NESS 91 In-Orbit Storage of NOAA-NESS Standby Satellites. Bruce Sharts and Chris Dunker, September 1977, 3 pp. (PB-283-078/AS)

NESS 92 Publications and Final Reports on Contracts and Grants, 1976. Catherine M. Frain (Compiler), August 1977, 11 pp. (PB-273-169/AS)

NESS 93 Computations of Solar Insolation at Boulder, Colorado. Joseph H. Pope, September 1977, 13 pp. (PB-273-679/AS)

NESS 94 A Report on the Chesapeake Bay Region Nowcasting Experiment. Roderick A. Scofield and Carl E. Weiss, December 1977, 52 pp. (PB-277-102/AS)

NESS 95 The TIROS-N/NOAA A-G Satellite Series. Arthur Schwalb, March 1978, 75 pp. (PB-283-859/AS)

NESS 96 Satellite Data Set for Solar Incoming Radiation Studies. J. Dan Tarpley, Stanley R. Schneider, J. Emmett Bragg, and Marshall P. Waters, III, May 1978, 36 pp. (PB-284-740/AS)

NESS 97 Publications and Final Reports on Contracts and Grants, 1977. Catherine M. Frain (Compiler), August 1978, 13 pp. (PB-287-855/AS)

NESS 98 Quantitative Measurements of Sea Surface Temperature at Several Locations Using the NOAA-3 Very High Resolution Radiometer. Laurence Breaker, Jack Klein, and Michael Pitts, September 1978, 28 pp. (PB-288-488/AS)

NESS 99 An Empirical Model for Atmospheric Transmittance Functions and Its Application to the NIMBUS-6 HIRS Experiment. P.G. Abel and W.L. Smith, NESS, and A. Arking, NASA, September 1978, 29 pp. (PB-288-487/AS)

NESS 100 Characteristics and Environmental Properties of Satellite-Observed Cloud Rows. Samuel K. Beckman (in consultation).

NESS 101 A Comparison of Satellite Observed Middle Cloud Motion With GATE Rawinsonde Data. Leroy D. Herman, January 1979, 13 pp. (PB-292-341/AS)

NESS 102 Computer Tracking of Temperature-Selected Cloud Patterns. Lester F. Hubert, January 1979, 15 pp. (PB-292-159/AS)

NESS 103 Objective Use of Satellite Data To Forecast Changes in Intensity of Tropical Disturbances. Carl O. Erickson, April 1979, 44 pp. (PB-298-915)

NESS 104 Publications and Final Reports on Contracts and Grants. Catherine M. Frain, (Compiler), September 1979. (PB80 122385)

NESS 105 Optical Measurements of Crude Oil Samples Under Simulated Conditions. Warren A. Hovis and John S. Knoll, October 1979, 20 pp. (PB80 120603)

NESS 106 An Improved Model for the Calculation of Longwave Flux at 11 m. P. G. Abel and A. Gruber, October 1979, 24 pp. (PB80 119431)

NESS 107 Data Extraction and Calibration of TIROS-N/NOAA Radiometers. Levin Lauritson, Gary J. Nelson, and Frank W. Porto, November 1979. (PB80 150824)

NESS 108 Publications and Final Reports on Contracts and Grants. Catherine M. Frain, (Compiler), August 1980. (PB81 124927)

NESS 109 Catalog of Products, Third Edition. Dennis C. Dismachek, Arthur L. Booth, and John A. Leese, April 1980, 130 pp. (PB81 106270)

NESS 110 GOES Data Collection Program. Merle Nelson, August 1980.

NESS 111 Earth Locating Image Data of Spin-Stabilized Geosynchronous Sateliites. Larry N. Hambrick and Dennis R. Phillips, August 1980. (PB81 120321)

NESS 112 Satellite Observations of Great Lakes Ice: Winter 1978-79. Jenifer Wartha-Clark, September 1980.

NESS 113 Satellite Identification of Surface Radiant Temperature Fields of Subpixel Resolution. Jeff Dozier, December 1980.

NOAA Technical Memorandum NESS 114

AN ATTITUDE PREDICTOR/TARGET SELECTOR

Bruce M. Sharts

Washington, D.C.
February 1981

UNITED STATES
DEPARTMENT OF COMMERCE
Malcolm Baldrige, Secretary

NATIONAL OCEANIC AND
ATMOSPHERIC ADMINISTRATION
James P. Walsh, Acting Administrator

National Earth Satellite Service
David S. Johnson,
Assistant Administrator

CONTENTS

FIGURES

TABLES

AN ATTITUDE PREDICTOR/TARGET SELECTOR

Bruce M. Sharts
National Earth Satellite Service

ABSTRACT. Accurate determination and prediction of the vehicle angular momentum vector is crucial to many satellite programs, particularly those that require the interpretation of satellite imagery.

A geostationary operational satellite program that services customers in near real time requires a spacecraft navigation capability that minimizes the number and/or magnitude of control pertubations to the orbit and attitude states. The accuracy of one's attitude determination and prediction process will profoundly affect this requirement.

The satellite mission may require that the vehicle be controlled to within some tolerance about a preferred attitude, i.e., orbit normal, ecliptic normal, or equatorial normal. Based on regular measurements of the angular momentum vector, a mechanism will be described for making attitude predictions and for optimizing the selection of attitude control targets for a geostationary satellite.

1. INTRODUCTION

The geostationary satellite program of the National Earth Satellite Service (NESS) involves spin stabilized vehicles that detect and transmit environmental imagery in the infrared and visible spectral regions in near real time. For these vehicles, the angular momentum vector is determined from the imagery.

At geostationary altitude, the major cause of precession of the vehicle angular momentum vector is solar radiation pressure. Given an attitude observation data base and an ephemeris for spacecraft and Sun, one may

make attitude predictions and target selections for long-term maneuver management.

Adequate short-term attitude predictions may be made by using the recent rate of change in the usual polar coordinates, right ascension and declination. The procedure is obvious; however the rate terms are, in general, no longer valid when the navigation analyst exercises attitude control by repositioning the angular momentum vector to a more optimum location. This procedure, therefore, cannot support an attitude control function. The navigation analyst requires an attitude predictor that can predict for extended periods from an arbitrary starting location.

Since the predictor described herein is based on empirical attitude data, it is desirable to examine attitude solutions for quality control. Having passed accepted standards, the solutions are added to a permanent attitude data base from which predictions are made.

The present NESS geostationary satellites exhibit a maximum daily precession magnitude of 35 arcsec and a minimum of 9 arcsec. On this scale, the polar coordinate system does not lend itself nicely to displaying one or two weeks of attitude solutions for the purpose of quality control and trend analysis. The navigation analyst requires that the attitude data points and corresponding predictions be displayed in a coordinate system of very high resolution. Such a coordinate system is the mercator coordinate system (described in detail in CSC 1973).

2. MATHEMATICAL MODELS

This section describes the fundamental coordinate systems and transformations used in the attitude predictor/target selector. Some coordinate transformations are defined as part of the model descriptions.

2.1 Coordinate Systems and Transformations

2.1.1 Inertial Equatorial Coordinate System

Figure 1 illustrates the inertial equatorial coordinate system (X_I,Y_I,Z_I). The X_I-Y_I plane is the equatorial plane. The X_I axis points toward the vernal equinox; the Z_I axis points north. The Y_I axis is such as to complete the orthogonal set. This coordinate system is referenced to the true-of-date epoch.

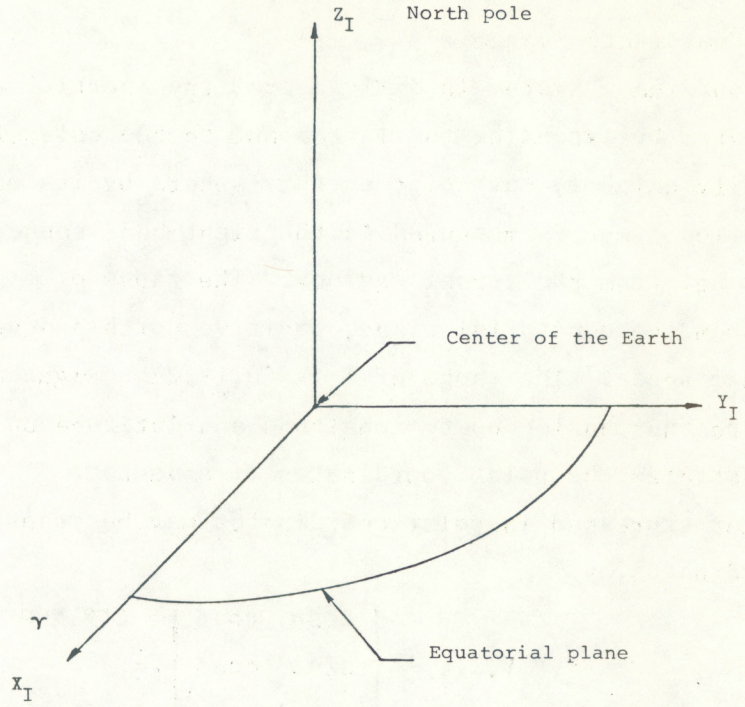

Figure 1.--Inertial equatorial coordinate system.

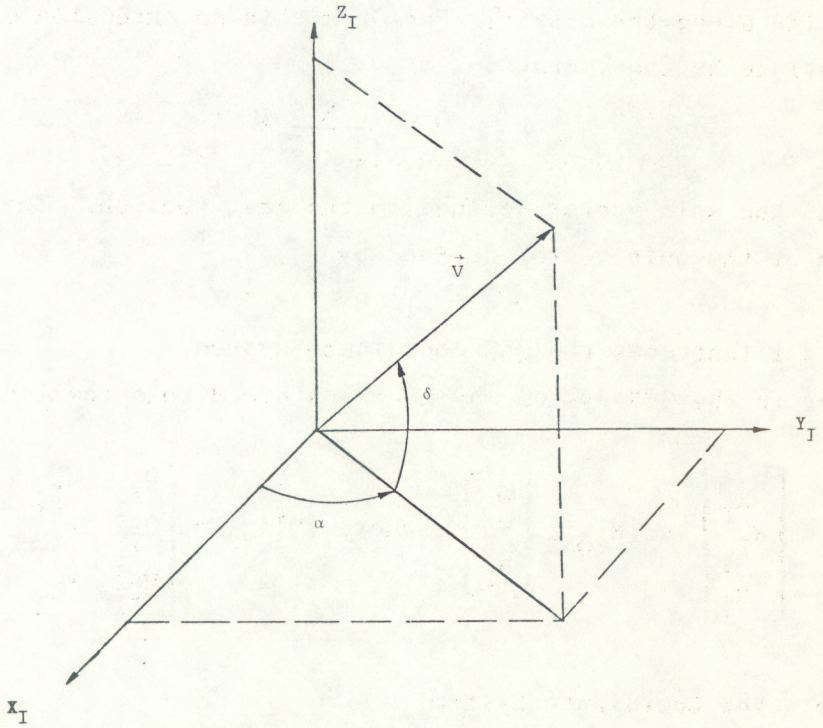

Figure 2.--Polar coordinate system.

2.1.2 Polar Coordinate System

The polar coordinate system is derived from the inertial equatorial coordinate system by extending the latter out to the celestial sphere. One may identify uniquely any point on this sphere by its right ascension α and declination δ. α is measured in the right-hand sense, in the equatorial plane, from the vernal equinox. The range of α is $(0,2\pi)$. δ is measured from the equatorial plane, positive north and negative south, in a meridional sense. The range of δ is $(0,\pm\pi/2)$. Right ascenion and declination are thus analogous to longitude and latitude on the Earth. Figure 2 illustrates the polar coordinates of a vector.

A unit vector expressed in polar coordinates may be transformed to inertial coordinates by

$$\hat{W}(X,Y,Z)_I = \begin{bmatrix} \cos\alpha & \cos\delta \\ \sin\alpha & \cos\delta \\ & \sin\delta \end{bmatrix}.$$

2.1.3 Sun-Spin (QES) Coordinate System

This coordinate system is constructed from the inertial vector to the Sun and the vehicle angular momentum (spin) vector. The unit vector to the Sun lies along the S axis. The Q axis is an extension of the unit vector defined by the operation

$$\hat{Q} = \frac{\hat{W} \times \hat{S}}{|\hat{W} \times \hat{S}|},$$

where $\hat{W}$ is the spin vector defined in the last section. The E axis is an extension of the unit vector defined by

$$\hat{E} = \hat{S} \times \hat{Q}.$$

Figure 3 illustrates the QES coordinate system.

A vector in the QES system may be transformed into the inertial system by

$$\begin{bmatrix} W_{X_I} \\ W_{Y_I} \\ W_{Z_I} \end{bmatrix} = [M]_{QES} \begin{bmatrix} W_Q \\ W_E \\ W_S \end{bmatrix}, \text{ where } [M]_{QES} = \begin{bmatrix} Q_{X_I} & E_{X_I} & S_{X_I} \\ Q_{Y_I} & E_{Y_I} & S_{Y_I} \\ Q_{Z_I} & E_{Z_I} & S_{Z_I} \end{bmatrix}.$$

2.1.4 Mercator Coordinate System

As with polar coordinates, a vector in the QES system may be defined in terms of two angles, theta and phi. Theta (θ) is measured in the right-hand

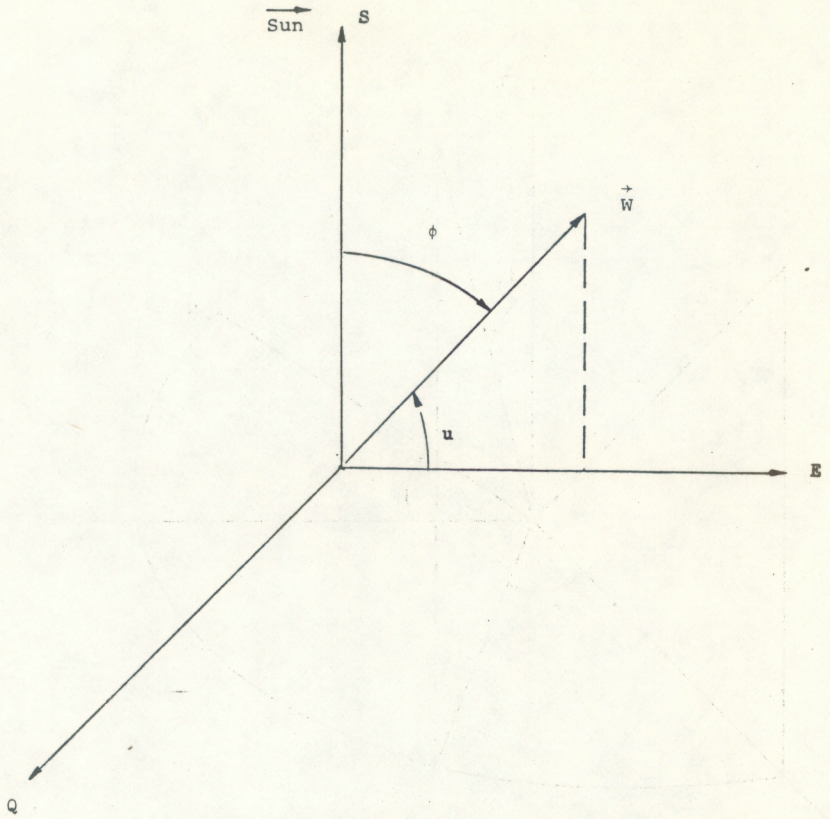

Figure 3.--QES coordinate system.

sense about the S axis, from the E axis to the projection of a vector onto the Q-E plane. For the purpose of prediction, the initial spin vector $\hat{W}_0$ is a known state at a known time. $\hat{W}_0$ and the Sun vector at that time $\hat{S}_0$ will form the epoch $(QES)_0$ coordinate system. In that system, $\theta_0 \equiv 0$. The -Q axis is an extension of the unit vector in the direction of $\hat{S}_0 \times \hat{W}_0$. Predicted spin vectors $\hat{W}_i$ are expressed in the $(QES)_0$ system to calculate

$$\hat{N}_i = \frac{\hat{S}_0 \times \hat{W}_i}{|\hat{S}_0 \times \hat{W}_i|} .$$

θ_i may then be calculated, $\theta_i = \cos^{-1}(-\hat{Q} \cdot \hat{N}_i)$.

Phi (ϕ) is the colatitude of the Sun, the angle between the spin vector and the line-of-sight vector to the Sun. ϕ is calculated as $\phi = \cos^{-1}(\hat{W}_i \cdot \hat{S}_i)$. $\pi/2 - \phi = u$ is the Sun angle, or solar latitude relative to a plane normal to the spin vector.

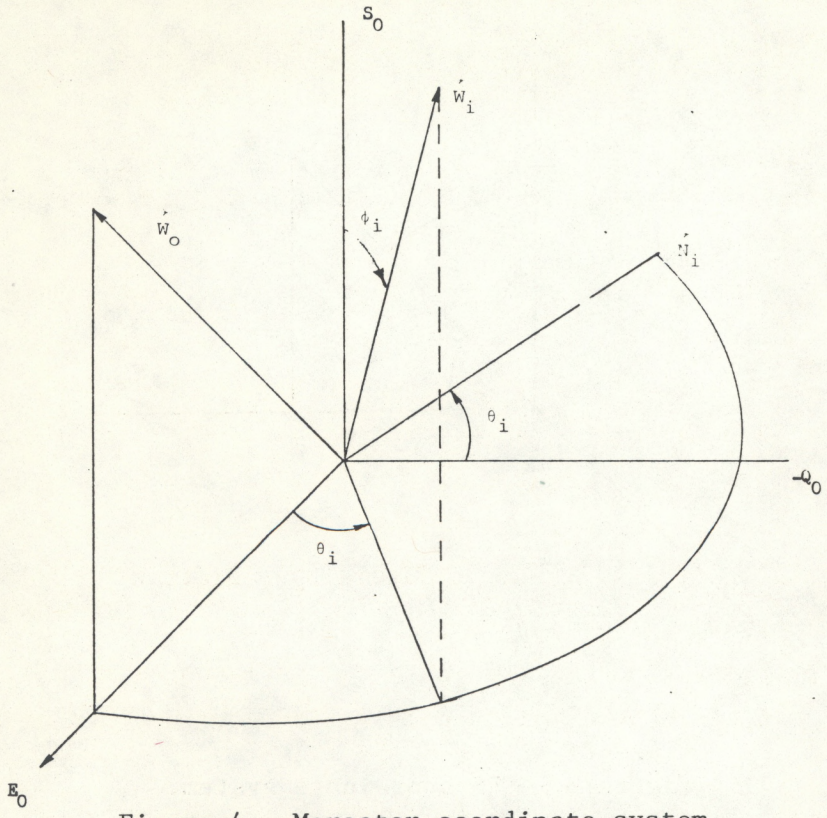

Figure 4.--Mercator coordinate system.

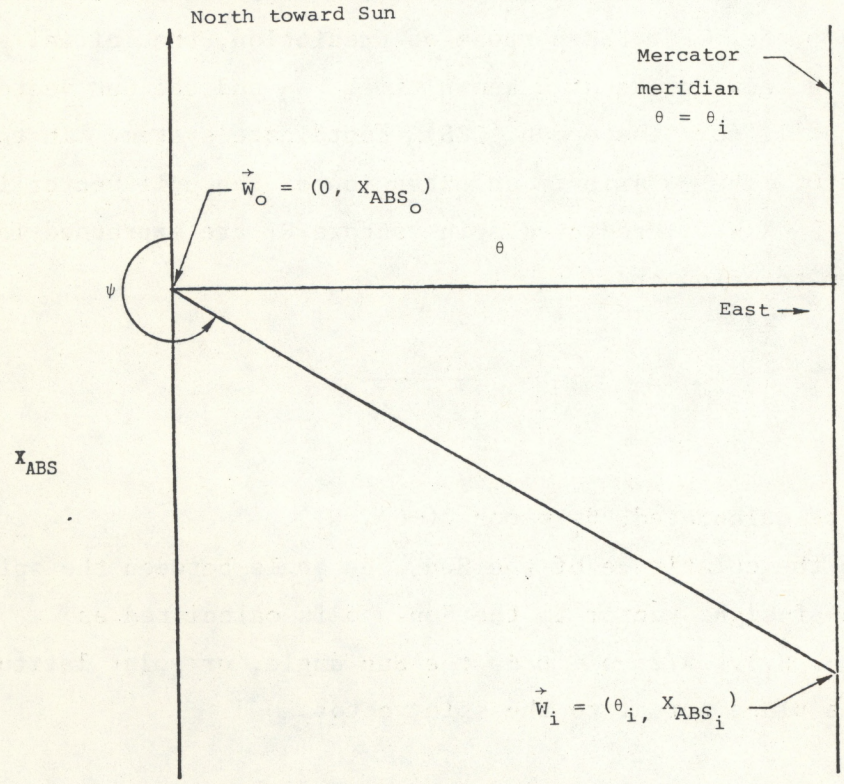

Figure 5.--Mercator projection.

The mercator coordinates of a vector are defined by θ and by $X_{abs} = -\ln [\tan(\phi_i/2)]$, where $\phi_i = \cos^{-1}(\hat{W}_i \cdot \hat{S}_0)$ and $\hat{W}_i$ is expressed in $(QES)_0$. X_{abs} is the mercator latitude and has the same polarity as u. Note that X_{abs} is not defined when the spin vector is parallel to the Sun vector. Figure 4 illustrates the angles that make up the mercator coordinates.

2.1.5 The Mercator Projection (CSC 1973)

Figure 5 shows two spin vectors, separated by a small precession angle, pointing out of the mercator projection plane. The precession direction has taken a heading angle ψ measured from a direction toward the Sun. With this definition of heading angle and knowledge that solar radiation pressure is along $-\hat{S}$, it is clear that $\psi \equiv (3/2)\pi$. The heading angle ψ may be thought of as the spin angle from the Sun vector projection onto the spin plane to the torque vector produced by radiation pressure.

2.1.6 $(QES)_f$ Coordinates

When attitude observations are added to the permanent attitude data base, one bit of information in each attitude record may be the quantity,

$$\dot{\tau}_i = \frac{\cos^{-1}(\hat{W}_i \cdot \hat{W}_{i-1})}{t_i - t_{i-1}} .$$

A plot of $\dot{\tau}$ vs. time will produce a waveform similar to that shown in figure 6 and will repeat itself essentially on an annual cycle. One may fit easily a polynomial to this data to obtain $\dot{\tau}$ as a function of time.

(CSC) 1973) discusses thoroughly the use of u, ψ, τ*, respectively, in a transformation from a given QES coordinate system to a final QES system such that the final spin vector is known. In this case, the final spin vector is the desired attitude prediction. Figure 7 illustrates the rotation angles and the initial, interim, and final coordinates. For clarity, the interim and final S axes are not shown. Note that the first two rotations orient the Q_2 axis normal to the predicted precession plane. The final

---

*(CSC 1973) uses κ in a maneuver model instead of τ.

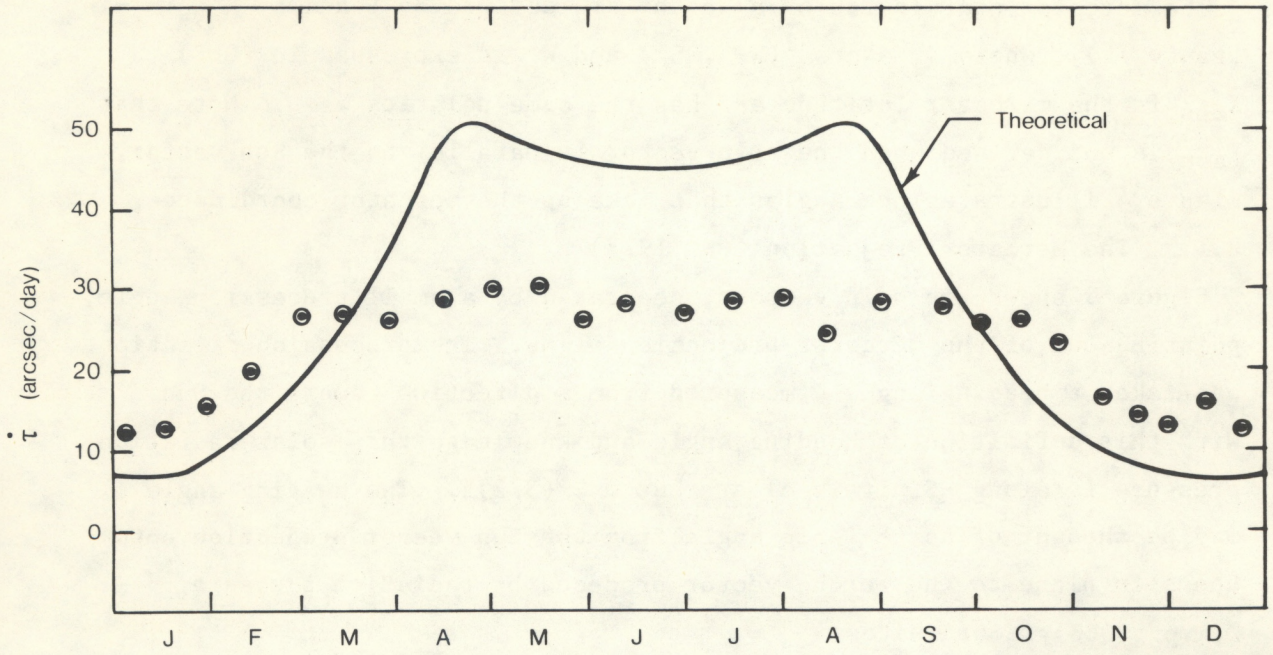

Figure 6.--Seasonal precession due to solar radiation pressure. (theoretical vs. observed).

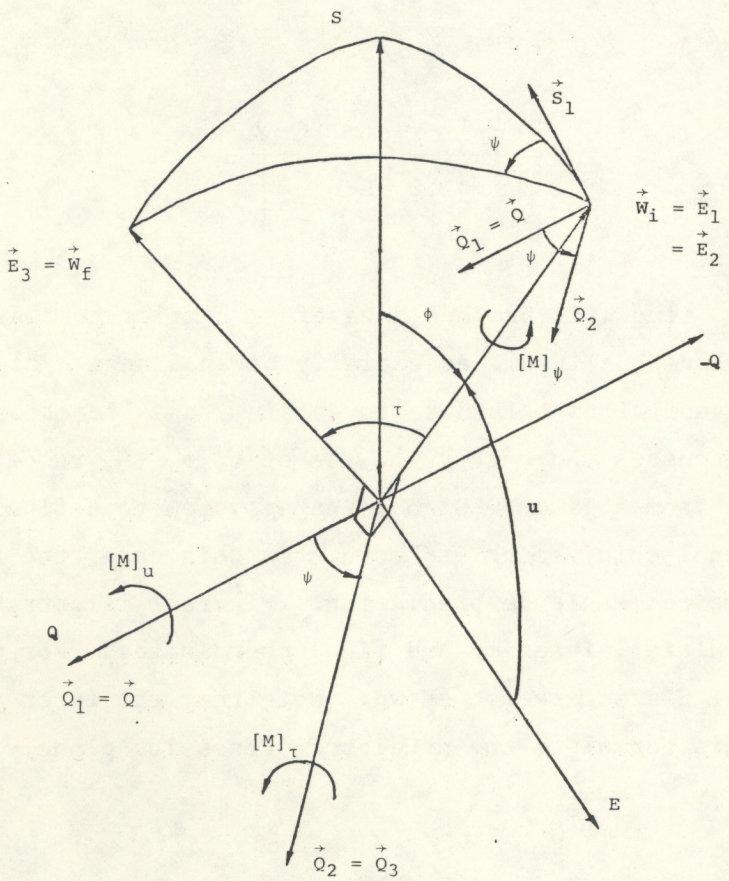

Figure 7.--W_f transformation.

rotation through the angle τ precesses the initial spin vector into the predicted spin vector. This $\hat{W}_f$ is the unit vector along the E_3 axis.

The requirement is to express $\hat{W}_f$ in the QES coordinate system from which it precessed. The transformation for this is

$$(\hat{W}_f)_{QES} = [M]^T_{\tau\psi u} \begin{bmatrix} 0 \\ 1 \\ 0 \end{bmatrix}, \text{ where } [M]_{\tau\psi u} = [M]_\tau \, [M]_\psi \, [M]_u \text{ and}$$

$$[M]_u = \begin{bmatrix} 1 & 0 & 0 \\ 0 & \cos u & \sin u \\ 0 & -\sin u & \cos u \end{bmatrix}, \quad [M]_\psi = \begin{bmatrix} \cos\psi & 0 & -\sin\psi \\ 0 & 1 & 0 \\ \sin\psi & 0 & \cos\psi \end{bmatrix}, \text{ and } [M]_\tau = \begin{bmatrix} 1 & 0 & 0 \\ 0 & \cos\tau & \sin\tau \\ 0 & -\sin\tau & \cos\tau \end{bmatrix}.$$

2.1.7 $(QES)_i$ to $(QES)_0$ Coordinate Transformation

Using the transformation of the last section, one may express the first attitude prediction in the $(QES)_0$ system. If inertial coordinates are desired, recall the transformation of section 2.1.3. To further propagate the attitude in time, one transforms a current Sun vector into the $(QES)_0$ system. This vector, along with the $\hat{W}_i$ just found, is used to form a $(QES)_i$ coordinate system. A transformation $[M]_o$ to the $(QES)_0$ system is defined as

$$[M]_0 = \begin{bmatrix} Q_1 & E_1 & S_1 \\ Q_2 & E_2 & S_2 \\ Q_3 & E_3 & S_3 \end{bmatrix},$$

where the $(QES)_k$, $k = 1,2,3$ are the $(QES)_i$ coordinate vectors expressed in the $(QES)_0$ system.

2.2 Attitude Predictor

Assuming that solar radiation pressure produces the attitude precession observed, one may integrate an arbitrary angular momentum vector stepwise in time. To summarize section 2 thus far, one creates an epoch $(QES)_0$ coordinate system, uses the angles u, ψ, τ to calculate an attitude prediction $\hat{W}_i$ at time t_i, uses $\hat{W}_i$ and $\hat{S}_i$ expressed in $(QES)_0$ to form $(QES)_i$, and uses u_i, ψ, τ_i to calculate W_{i+1} for the next integration cycle. The navigation analyst may use the attitude predictions to effect quality control on attitude observations taken subsequent to $\hat{W}_0$. Periodically, one may update the attitude data base with acceptable observations, so that the $\dot{\tau}$ polynomial will be current.

2.3 Target Selection

One task of the navigation analyst is to control the vehicle attitude to within a specified boundary about a preferred orientation. Proper control management may require that the number and magnitude of control maneuvers be as small as possible. Typical preferred orientations were mentioned earlier. The following discussions will assume an orbit normal attitude; however, the model is easily adapted to other preferred orientations.

The basic goals of the target selector are to determine when a control maneuver is necessary and to select the target attitude such that the time to the next control maneuver is maximized. Spacecraft ephemeris and the attitude predictor are used to achieve these goals.

2.3.1 Orbit Normal

The spacecraft ephemeris will give position and velocity vectors at specified time increments. In this case, the unit preferred attitude vector is

$$\hat{W}_N = \frac{\hat{R} \times \hat{V}}{|\hat{R} \times \hat{V}|} ,$$

where $\hat{R}$ and $\hat{V}$ are position and velocity vectors, respectively.

2.3.2 TAR Coordinate System

This coordinate system will simplify the target selection process. Figures 8 and 9 illustrate the preferred attitude, its boundary, and the TAR coordinate system.

The R axis is an extension of the $\hat{W}_N$ vector. The T axis is an extension of the unit vector from the operation,

$$\hat{T} = \frac{\hat{W}_N \times \hat{Z}_I}{|\hat{W}_N \times \hat{Z}_I|} ,$$

where $\hat{Z}_I$ is the unit vector along the inertial Z_I axis. The A axis is an extension of the unit vector defined by $\hat{A} = \hat{W}_N \times \hat{T}$.

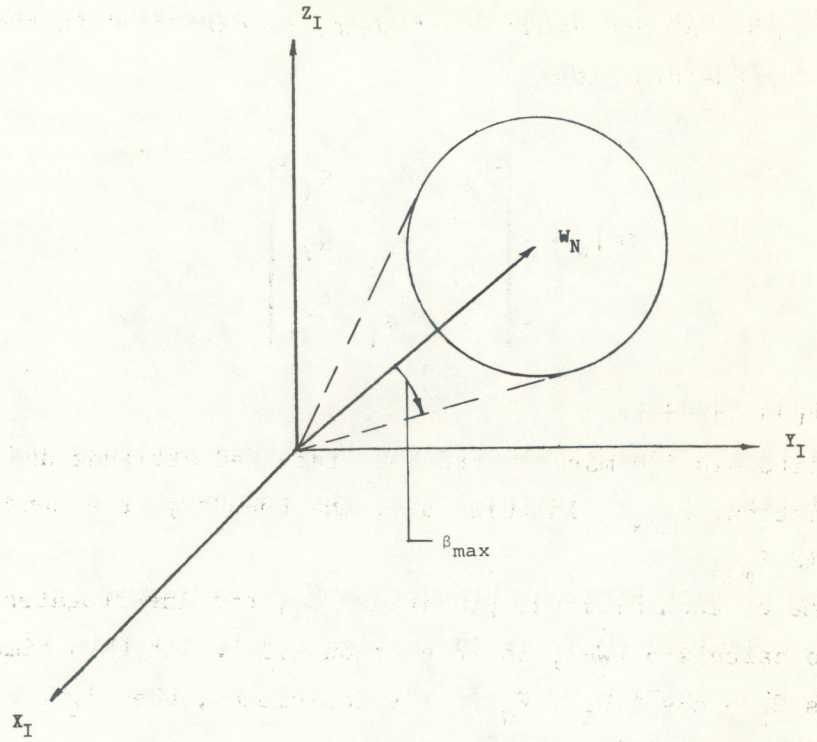

Figure 8.--β_{max} cone.

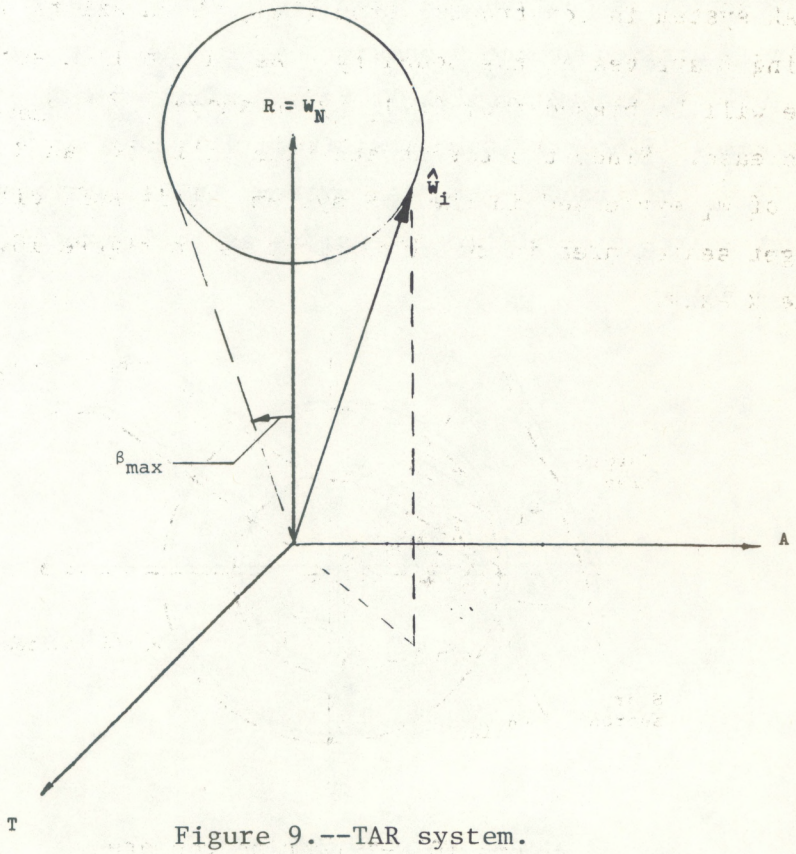

Figure 9.--TAR system.

A vector in the TAR coordinate system may be expressed in the inertial system by the transformation,

$$[M]_N = \begin{bmatrix} T_{X_I} & A_{X_I} & R_{X_I} \\ T_{Y_I} & A_{Y_I} & R_{Y_I} \\ 0 & A_{Z_I} & R_{Z_I} \end{bmatrix} .$$

2.3.3 Attitude Boundary

The satellite mission may dictate the preferred attitude and the maximum allowed deviation, β_{max}. In this case, the boundary is a cone about $\hat{W}_N$ of half-angle β_{max}.

At the time of each attitude prediction $\hat{W}_i$, one interrogates the spacecraft ephemeris to calculate $(\hat{W}_N)_i$ as in section 2.3.1. At this time, the deviation is $\beta_i = \cos^{-1}(\hat{W}_i \cdot \hat{W}_{N_i})$. By definition, when $\beta_i \geq \beta_{max}$, a maneuver control condition exists.

2.3.4 Target Search

The TAR system is constructed from $(\hat{W}_N)_i$ which exists at the time the increasing β arrives at the boundary. As in the last section, the target attitude will be biased from $(\hat{W}_N)_i$ by an amount, $\beta = \beta_{max}$, such that β will decrease. Since the target attitude will have an R component equal to that of $\hat{W}_i$ expressed in the TAR system, it is sufficient to illustrate the target search area in two dimensions as in figure 10. The view is down the R axis.

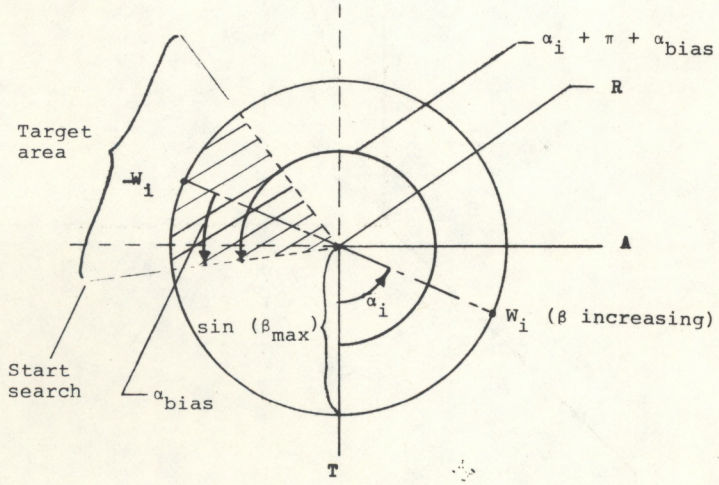

Figure 10.--Target search area.

The remaining two components of $\hat{W}_T$ may be approximated by the negative of those of $(\hat{W}_i)_{T,A}$. For a computer program, it is useful to bias the initial search to one "side" of $(-W_i)_{T,A}$ as shown in figure 10. One then steps through the target area seeking the starting vector that will maximize the time until the next arrival at the boundary.

Any precession of the preferred attitude is accounted for in section 2.3.4.

3. RESULTS

Figures 11 and 12 show plots of attitude predictions and corresponding observations in mercator coordinates. The data shown span a period of about three weeks, during which the only perturbation to the angular momentum is assumed to be solar radiation pressure. With these plots, the analyst is able to observe the following:

a. Individual solution fit relative to the observed and predicted trend. (See figure 11, data point 7.)

b. Biases due to updated orbital parameters used in the attitude deterministic process. (See data points 8 & 12, figure 11, and 7 & 11, figure 12.)

c. Biases due to modeling errors, unmodeled perturbing forces, i.e., gravity gradient, magnetic fields, etc.

The plots shown are with respect to an epoch QES coordinate system based on the attitude measurement of April 12, 1979. The worst-case error of prediction to associated observation is 0.0089 degrees for data point 7 on April 24, 1979.

As in section 2.1.6, the navigation analyst may decide to downgrade the quality of data point 7 when adding this data set to the permanent attitude file for subsequent predictions.

Figure 12 is a repeat of figure 11, excluding data point 7.

Table 1 is a listing of polar and mercator coordinates and the error between the observations and predictions shown in figure 11. The date line contains the observation, if one exists. The next line contains the prediction for that date and the error. Because epoch is the starting point for predictions, there is no prediction listed for epoch.

4. CONCLUSION

Navigation analysts in NESS have been using the described attitude predictor/target selector for about 5 years. It has become an invaluable

tool in the maneuver management process. Table 1 shows the short-term (3 weeks) prediction accuracy. With this accuracy, the navigation analyst has confidence in scheduling attitude maneuver dates, times, and targets for several weeks in advance.

The precession behavior shown in figure 6 is typical of all vehicles in a given series. Therefore, for a new vehicle in the series, the analyst need only couple one attitude solution to the precession history of any prior vehicle to make reasonably accurate predictions and target selections. For the first vehicle of a series, the analyst may use the predicted precession behavior supplied by the satellite vendor. Figure 6 shows such data supplied by Philco-Ford (Lehner 1971).

5. REFERENCES

CSC, 1973: Synchronous meteorological satellite (SMS) maneuver control program (SMSMAN) task specification. Computer Sciences Corporation, Washington, D.C.

Lehner, J., 1971: Revised solar pressure analysis. Intracompany correspondence, Philco-Ford Corporation, Palo Alto, Calif.

Table 1.--Observations/predictions of figure 11

Data point (figure 11)	Date	α	δ	X_{ABS}	θ	Error (degrees)
1 (Epoch)	790412	349.06383	-89.52718	-0.139650	0.000000	
	790413	349.91462	-89.53127	-0.139650	0.008199	
2	790414	350.69731	-89.53666	-0.139677	0.016462	
		350.77231	-89.53537	-0.139652	0.016362	0.0009
3	790415	351.67814	-89.54093	-0.139677	0.025519	
		351.63708	-89.53947	-0.139657	0.024545	0.00015
	790416	352.50914	-89.54359	-0.139664	0.032705	
4	790417	352.74312	-89.54464	-0.139665	0.034865	
		353.38867	-89.54771	-0.139673	0.040871	0.0059
5	790418	353.81468	-89.54973	-0.139679	0.044810	
		354.27587	-89.55183	-0.139684	0.049022	0.0041

Table 1.--Observations/predictions of figure 11 (Cont'd)

Data point (figure 11)	Date	α	δ	X_{ABS}	θ	Error (degrees)
6	790419	354.64518	-89.55475	-0.139709	0.052907	
		355.17097	-89.55596	-0.139698	0.057161	0.0042
	790420					
		356.07416	-89.56009	-0.139714	0.065288	
	790421					
		356.98567	-89.56423	-0.139732	0.073399	
	790422					
		357.90574	-89.56836	-0.139753	0.081492	
	790423					
		358.83458	-89.57250	-0.139776	0.089564	
7	790424	359.47345	-89.56795	-0.139671	0.092466	
		359.77245	-89.57664	-0.139801	0.097614	0.0089
8	790425	0.79449	-89.57786	-0.139777	0.105203	
		0.71958	-89.58077	-0.139829	0.105642	0.0029
9	790426	1.48801	-89.58361	-0.139844	0.111918	
		1.67624	-89.58491	-0.139858	0.113639	0.0019
	790427					
		2.64269	-89.58904	-0.139891	0.121611	
10	790428	3.61065	-89.59204	-0.139906	0.129169	
		3.61919	-89.59317	-0.139925	0.129550	0.0012
11	790429	4.76412	-89.59650	-0.139943	0.138327	
		4.60602	-89.59729	-0.139962	0.137454	0.0013
12	790430	5.58700	-89.59565	-0.139902	0.143776	
		5.60347	-89.60141	-0.140000	0.145325	0.0057
13	790501	6.69080	-89.60211	-0.139981	0.152904	
		6.61182	-89.60553	-0.140042	0.153155	0.0034
14	790502	7.10388	-89.60444	-0.140009	0.156247	
		7.63139	-89.60963	-0.140085	0.160948	0.0063
15	790503	8.66761	-89.61141	-0.140090	0.168276	
		8.66248	-89.61373	-0.140131	0.168697	0.0023

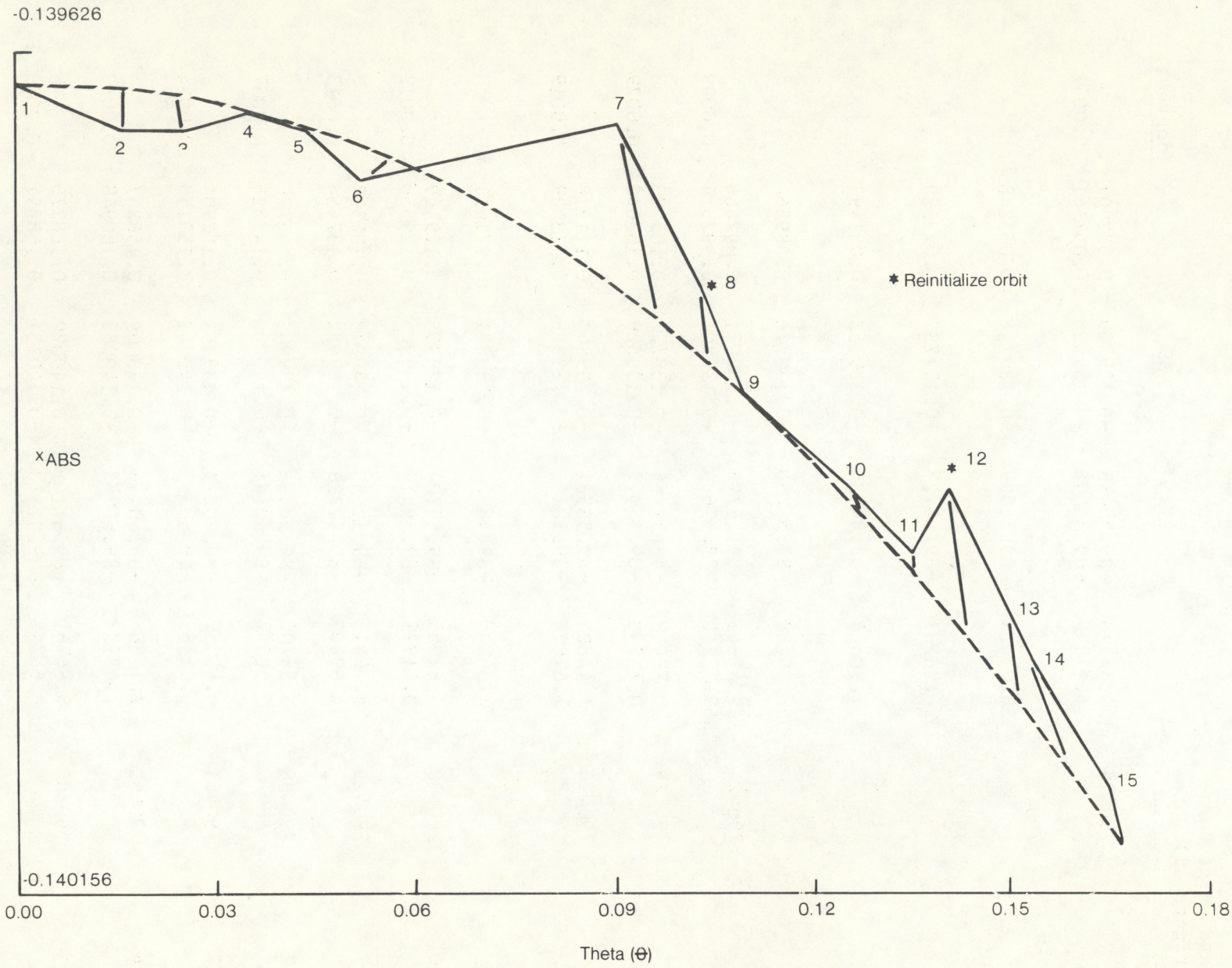

Figure 11.--Mercator plot (unedited).

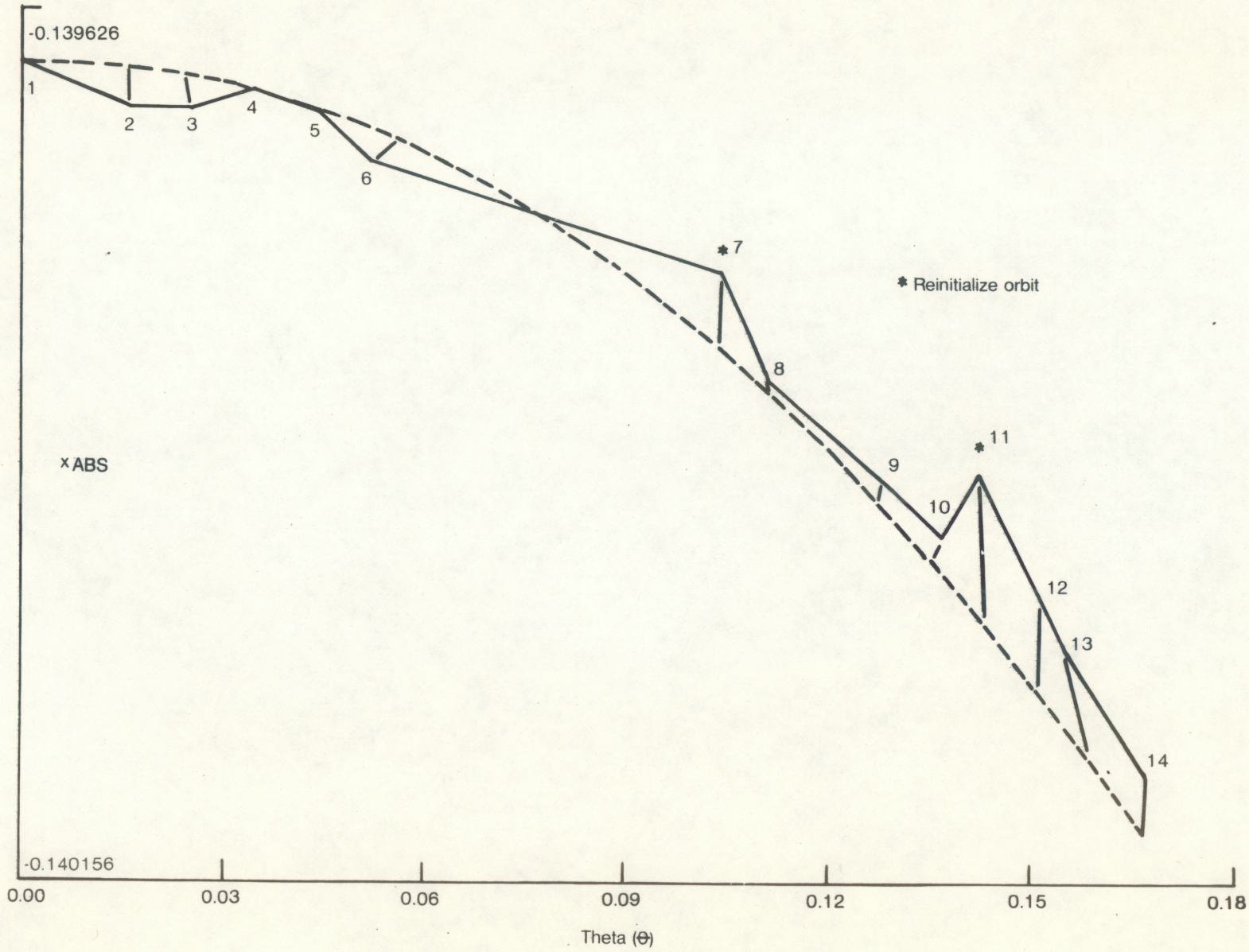

Figure 12.--Mercator plot (edited)

(Continued from inside front cover)

NESS 87 Atlantic Tropical and Subtropical Cyclone Classifications for 1976. D. C. Gaby, J. B. Lushine, B. M. Mayfield, S. C. Pearce, K.O. Poteat, and F. E. Torres, April 1977, 13 pp. (PB-269-674/AS)

NESS 88 National Environmental Satellite Service Catalog of Products. Dennis C. Dismachek (Editor), June 1977, 102 pp. (PB-271-315/AS)

NESS 89 A Laser Method of Observing Surface Pressure and Pressure-Altitude and Temperature Profiles of the Troposphere From Satellites. William L. Smith and C. M. R. Platt, July 1977, 38 pp. (PB-272-660/AS)

NESS 90 Lake Erie Ice: Winter 1975-76. Jenifer H. Wartha, August 1977, 68 pp. (PB-276-386/AS)

NESS 91 In-Orbit Storage of NOAA-NESS Standby Satellites. Bruce Sharts and Chris Dunker, September 1977, 3 pp. (PB-283-078/AS)

NESS 92 Publications and Final Reports on Contracts and Grants, 1976. Catherine M. Frain (Compiler), August 1977, 11 pp. (PB-273-169/AS)

NESS 93 Computations of Solar Insolation at Boulder, Colorado. Joseph H. Pope, September 1977, 13 pp. (PB-273-679/AS)

NESS 94 A Report on the Chesapeake Bay Region Nowcasting Experiment. Roderick A. Scofield and Carl E. Weiss, December 1977, 52 pp. (PB-277-102/AS)

NESS 95 The TIROS-N/NOAA A-G Satellite Series. Arthur Schwalb, March 1978, 75 pp. (PB-283-859/AS)

NESS 96 Satellite Data Set for Solar Incoming Radiation Studies. J. Dan Tarpley, Stanley R. Schneider, J. Emmett Bragg, and Marshall P. Waters, III, May 1978, 36 pp. (PB-284-740/AS)

NESS 97 Publications and Final Reports on Contracts and Grants, 1977. Catherine M. Frain (Compiler), August 1978, 13 pp. (PB-287-855/AS)

NESS 98 Quantitative Measurements of Sea Surface Temperature at Several Locations Using the NOAA-3 Very High Resolution Radiometer. Laurence Breaker, Jack Klein, and Michael Pitts, September 1978, 28 pp. (PB-288-488/AS)

NESS 99 An Empirical Model for Atmospheric Transmittance Functions and Its Application to the NIMBUS-6 HIRS Experiment. P.G. Abel and W.L. Smith, NESS, and A. Arking, NASA, September 1978, 29 pp. (PB-288-487/AS)

NESS 100 Characteristics and Environmental Properties of Satellite-Observed Cloud Rows. Samuel K. Beckman (in consultation).

NESS 101 A Comparison of Satellite Observed Middle Cloud Motion With GATE Rawinsonde Data. Leroy D. Herman, January 1979, 13 pp. (PB-292-341/AS)

NESS 102 Computer Tracking of Temperature-Selected Cloud Patterns. Lester F. Hubert, January 1979, 15 pp. (PB-292-159/AS)

NESS 103 Objective Use of Satellite Data To Forecast Changes in Intensity of Tropical Disturbances. Carl O. Erickson, April 1979, 44 pp. (PB-298-915)

NESS 104 Publications and Final Reports on Contracts and Grants. Catherine M. Frain, (Compiler), September 1979. (PB80 122385)

NESS 105 Optical Measurements of Crude Oil Samples Under Simulated Conditions. Warren A. Hovis and John S. Knoll, October 1979, 20 pp. (PB80 120603)

NESS 106 An Improved Model for the Calculation of Longwave Flux at 11 m. P. G. Abel and A. Gruber, October 1979, 24 pp. (PB80 119431)

NESS 107 Data Extraction and Calibration of TIROS-N/NOAA Radiometers. Levin Lauritson, Gary J. Nelson, and Frank W. Porto, November 1979. (PB80 150824)

NESS 108 Publications and Final Reports on Contracts and Grants. Catherine M. Frain, (Compiler), August 1980. (PB81 124927)

NESS 109 Catalog of Products, Third Edition. Dennis C. Dismachek, Arthur L. Booth, and John A. Leese, April 1980, 130 pp. (PB81 106270)

NESS 110 GOES Data Collection Program. Merle Nelson, August 1980.

NESS 111 Earth Locating Image Data of Spin-Stabilized Geosynchronous Satelliites. Larry N. Hambrick and Dennis R. Phillips, August 1980. (PB81 120321)

NESS 112 Satellite Observations of Great Lakes Ice: Winter 1978-79. Jenifer Wartha-Clark, September 1980.

NESS 113 Satellite Identification of Surface Radiant Temperature Fields of Subpixel Resolution. Jeff Dozier, December 1980.

NOAA SCIENTIFIC AND TECHNICAL PUBLICATIONS

The National Oceanic and Atmospheric Administration was established as part of the D of Commerce on October 3, 1970. The mission responsibilities of NOAA are to assess the socioeco t of natural and technological changes in the environment and to monitor and predict the state of th , the oceans and their living resources, the atmosphere, and the space environment of the Earth.

The major components of NOAA regularly produce various types of scientific and techn tion in the following kinds of publications:

PROFESSIONAL PAPERS — Important definitive research results, major techniques, and special investigations.

CONTRACT AND GRANT REPORTS — Reports prepared by contractors or grantees under NOAA sponsorship.

ATLAS — Presentation of analyzed data generally in the form of maps showing distribution of rainfall, chemical and physical conditions of oceans and atmosphere, distribution of fishes and marine mammals, ionospheric conditions, etc.

TECHNICAL SERVICE PUBLICATIONS — Reports containing data, observations, instructions, etc. A partial listing includes data serials; prediction and outlook periodicals; technical manuals, training papers, planning reports, and information serials; and miscellaneous technical publications.

TECHNICAL REPORTS — Journal quality with extensive details, mathematical developments, or data listings.

TECHNICAL MEMORANDUMS — Reports of preliminary, partial, or negative research or technology results, interim instructions, and the like.

Information on availability of NOAA publications can be obtained from:

ENVIRONMENTAL SCIENCE INFORMATION CENTER (D822)
ENVIRONMENTAL DATA AND INFORMATION SERVICE
NATIONAL OCEANIC AND ATMOSPHERIC ADMINISTRATION
U.S. DEPARTMENT OF COMMERCE

6009 Executive Boulevard
Rockville, MD 20852

NOAA--S/T 80-302